Penalization of Robin boundary conditions

Bouchra Bensiali, Guillaume Chiavassa, Jacques Liandrat

Penalization of Robin boundary conditions

Bouchra Bensiali[a,*], Guillaume Chiavassa[b], Jacques Liandrat[c]

[a] *Aix Marseille Université, CNRS, Centrale Marseille, M2P2 UMR 7340, 13451, Marseille, France*
[b] *Centrale Marseille, CNRS, Aix Marseille Université, M2P2 UMR 7340, 13451, Marseille, France*
[c] *Centrale Marseille, CNRS, Aix Marseille Université, I2M UMR 7373, 13453, Marseille, France*

Abstract

This paper is devoted to the mathematical analysis of a method based on fictitious domain approach. Boundary conditions of Robin type (also known as Fourier boundary conditions) are enforced using a penalization method. A complete description of the method and a full analysis are provided for univariate elliptic and parabolic problems using finite difference approximation. Numerical evidence of the predicted estimations is provided as well as numerical results for a nonlinear problem and a first extension of the method in the bivariate situation is proposed.

Keywords: fictitious domain methods, penalization, Robin boundary conditions, finite difference methods
2010 MSC: Primary 65M85, 65N85, 65M06, 65N06

1. Introduction

This paper is devoted to the definition and analysis of a finite difference fictitious domain method where the boundary conditions of Robin type are enforced using a penalization method. As for all fictitious domain methods, the initial problem with solution u and raised on a domain ω is solved using a larger but simpler domain $\Omega \supset \omega$. In penalization methods, the new problem defined on Ω is parametrized by η defined in such a way that its solution u_η restricted to ω converges, when η goes to zero, towards u the solution of the initial problem.

Penalization has been introduced by Arquis and Caltagirone [5] in the 80's and analyzed by Angot et al. [4] for incompressible Navier-Stokes equations. Various theoretical results have been established for Dirichlet boundary conditions, in the case of parabolic [18] or hyperbolic [22, 13, 14, 10] equations. The main advantage of penalization methods stands in allowing the numerical resolution of the problem in an obstacle-free simple domain. There, the use of a Cartesian mesh is possible and different numerical methods including pseudo-spectral methods [18], finite differences/volumes [4, 20, 22] and wavelets [26, 27, 19] can be implemented efficiently to approximate the solution.

This paper can be considered as a continuation of [16] where Dirichlet boundary conditions were considered. The scope of that paper was the modeling of the plasma-wall interaction

*Corresponding author. Tel: +33 4 91 11 85 21; Fax: +33 4 91 11 85 02.
Email addresses: bensiali@l3m.univ-mrs.fr (Bouchra Bensiali), gchiavassa@centrale-marseille.fr (Guillaume Chiavassa), jliandrat@centrale-marseille.fr (Jacques Liandrat)

in the region of a tokamak called Scrape-Off Layer (SOL), where magnetic field lines are open and intercept solid obstacles. A volume penalization method has been proposed to take into account the boundary conditions associated with a hyperbolic model system for the density and the momentum of the plasma through a magnetic field line in the SOL region. A modification of this method has been given in [3] to eliminate the presence of an artificial boundary layer. Enriching the physical model of the edge plasma requires adding the evolution of ionic and electronic temperatures. These quantities are modeled by parabolic equations with boundary conditions of Neumann or Robin types. This extension of the physical model is the starting point and the initial motivation of the present work, since few penalization methods for this type of conditions exist in the literature, see for instance [2, 24, 25, 17]. As in [16], univariate problems are first considered. For the theoretical analysis of the penalization, the initial problem is raised on $\omega =]0,1[$ and the fictitious domain is defined as $\Omega =]0,2[$. For the numerical approximation, a more realistic situation inspired by tokamak geometry is considered: the domain ω is $]0,x_l[\cup]x_r,1[$ and $\Omega =]0,1[$ with $0 < x_l < x_r < 1$.

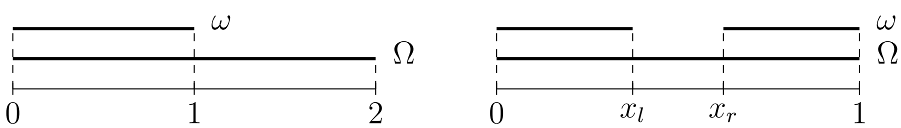

Figure 1: Left: geometrical domain for theoretical analysis. Right: geometrical domain used for applications. In both cases ω is the initial domain, Ω is the fictitious domain.

The paper is organized as follows: Section 2 is devoted to elliptic equations. The penalized problem is introduced and existence, uniqueness and convergence of the solution in regard to penalization parameter are established. Numerical approximation of the problem using finite differences is defined and analyzed in Section 2.6. Convergence and stability analysis are provided and illustrated by various numerical tests. Parabolic equations are considered in Section 3 where a time discretization followed by space discretization are used. The analysis is performed and illustrated by various simulations. Section 4 is devoted to numerical tests for a nonlinear problem describing the temperature in the plasma of a tokamak close to an obstacle. A first application of the method to the bivariate situation is also presented.

2. Elliptic equation

2.1. Definition of the problem

An archetype of elliptic partial differential equations with Robin boundary conditions is the so called reaction-diffusion equation

$$\begin{cases} -\Delta u + u = f & \text{in } \omega \\ \dfrac{\partial u}{\partial n} + \alpha u = g & \text{on } \partial\omega, \end{cases}$$

where ω is a given smooth bounded open set in $\mathbb{R}^D$, n is the outward-pointing unit normal vector on the boundary $\partial\omega$, $f \in L^2(\omega)$, $g \in L^2(\partial\omega)$ and $\alpha \geq 0$ are given. The case $\alpha = 0$ corresponds to Neumann boundary conditions. The Lax-Milgram theorem [1, 11] provides the existence and uniqueness of the solution $u \in H^1(\omega)$ of its weak formulation. In the particular case $D = 1$ and $\omega =]0,1[$, the problem reads

$$\begin{cases} -u'' + u = f \quad \text{in }]0,1[\\ -u'(0) + \alpha u(0) = g(0), \ u'(1) + \alpha u(1) = g(1). \end{cases} \tag{2.1}$$

The unique solution $u \in H^1(]0,1[)$ of the weak formulation of (2.1) is in fact in $H^2(]0,1[)$ taking into account that $u'' = u - f \in L^2(]0,1[)$. It follows using the Sobolev embedding $H^2(]0,1[) \hookrightarrow C^1([0,1])$ that $u \in C^1([0,1])$ and, if $f \in C^0([0,1])$ that $u \in C^2([0,1])$.

As presented on Figure 1 left, $\Omega =]0,2[$ is used to define a penalized problem associated with (2.1). Denoting χ the characteristic function of $\Omega \setminus \bar{\omega} =]1,2[$ and introducing a real parameter $\eta > 0$, a new problem raised on Ω with Robin boundary conditions at the boundary points reads

$$\begin{cases} -u_\eta'' + u_\eta + \dfrac{\chi}{\eta}\big(u_\eta' + \alpha u_\eta - g(1)\big) = (1-\chi) f \quad \text{in }]0,2[\\ -u_\eta'(0) + \alpha u_\eta(0) = g(0), \ u_\eta'(2) + \alpha u_\eta(2) = g(1). \end{cases} \tag{2.2}$$

When $x \in]0,1[$, $\chi(x) = 0$ and we recover the equation of (2.1) with the Robin condition at $x = 0$ unchanged. When $x \in]1,2[$, $\chi(x) = 1$, and using a small value of η implies that the leading term in the first equation of (2.2) is $\frac{1}{\eta}(u_\eta' + \alpha u_\eta - g(1))$ which imposes $u_\eta' + \alpha u_\eta - g(1) \approx 0$. We therefore recover, at least formally, the boundary conditions of (2.1).

Remark 2.1. Boundary conditions at $x = 2$ have been set to Robin type but different conditions could be enforced at this point.

In the following sections, we prove that this penalized problem (2.2) is well-posed in its weak form:

$$\left| \begin{array}{l} \text{Find } u_\eta \in H^1(]0,2[) \text{ such that } \forall v \in H^1(]0,2[) \\ \displaystyle\int_0^2 \Big(u_\eta' v' + u_\eta v + \frac{\chi}{\eta}(u_\eta' + \alpha u_\eta) v \Big)\, dx + \alpha\big(u_\eta(0)v(0) + u_\eta(2)v(2)\big) \\ \displaystyle\qquad\qquad = \int_0^2 \Big((1-\chi) f v + \frac{\chi}{\eta} g(1) v \Big)\, dx + \big(g(0)v(0) + g(1)v(2)\big), \end{array} \right. \tag{2.3}$$

and that its unique solution u_η tends, when η goes to 0, to a function $\bar{u}$ whose restriction to $]0,1[$ coincides with u the solution of the initial problem (2.1).

2.2. Existence and uniqueness

The coercivity of the bilinear form associated with the weak formulation (2.3) is not satisfied for all $\eta > 0$, and the Lax-Milgram theorem can not be applied. We have the following:

Lemma 2.2. *For all $\eta > 0$, there exists a unique solution $u_\eta \in H^1(]0,2[)$ of the weak formulation* (2.3) *of the penalized problem* (2.2)*. In addition, $u_\eta \in C^1([0,2])$.*

Proof. We first establish the regularity result. If $u_\eta \in H^1(]0,2[)$ is solution of the penalized problem (2.2) in its weak form (2.3) then $u_\eta \in H^2(]0,2[) \hookrightarrow C^1([0,2])$. We therefore seek a solution of class C^1 and looking at the equations satisfied in $]0,1[$ and $]1,2[$ respectively, u_η is of the form

$$u_\eta(x) = \begin{cases} \lambda_1 e^{x} + \mu_1 e^{-x} + u(x) & \text{if } x \in]0,1[\\ \lambda_2 e^{r_1 x} + \mu_2 e^{r_2 x} + \dfrac{g(1)}{\eta+\alpha} & \text{if } x \in]1,2[, \end{cases} \tag{2.4}$$

where

$$r_1 = \frac{1}{2}\left(\frac{1}{\eta} + \sqrt{\frac{1}{\eta^2} + 4\left(1+\frac{\alpha}{\eta}\right)}\right) \quad \text{and} \quad r_1 r_2 = -\left(1+\frac{\alpha}{\eta}\right).$$

Taking into account the Robin boundary conditions at $x = 0$ and $x = 2$ as well as the continuity of u_η and its derivative at $x = 1$, leads to the following linear system:

$$\begin{pmatrix} \alpha-1 & \alpha+1 & 0 & 0 \\ 0 & 0 & (\alpha+r_1)e^{2r_1} & (\alpha+r_2)e^{2r_2} \\ e & e^{-1} & -e^{r_1} & -e^{r_2} \\ e & -e^{-1} & -r_1 e^{r_1} & -r_2 e^{r_2} \end{pmatrix} \begin{pmatrix} \lambda_1 \\ \mu_1 \\ \lambda_2 \\ \mu_2 \end{pmatrix} = \begin{pmatrix} 0 \\ g(1) - \alpha\frac{g(1)}{\eta+\alpha} \\ \frac{g(1)}{\eta+\alpha} - u(1) \\ \alpha u(1) - g(1) \end{pmatrix}. \tag{2.5}$$

Its matrix M satisfies $\det(M) = e^{(-1+r_1+r_2)}(A + \alpha B + \alpha^2 C)$ with $\alpha \geq 0$ and

$$\begin{aligned} A &= (e^2-1)(r_1 e^{r_1} - r_2 e^{r_2}) + (1+e^2) r_1 r_2 (e^{r_2} - e^{r_1}), \\ B &= (1+e^2)(e^{r_1} + e^{r_2})(r_1 - r_2) + (e^2-1)(r_1 r_2 - 1)(e^{r_2} - e^{r_1}), \\ C &= (e^2-1)(r_1 e^{r_2} - r_2 e^{r_1}) + (1+e^2)(e^{r_1} - e^{r_2}). \end{aligned}$$

Since $r_1 > 0$ and $r_2 = -(1+\frac{\alpha}{\eta})/r_1 < 0$, we have $r_1 r_2 < 0$, $r_1 > r_2$ and $e^{r_1} > e^{r_2}$. Therefore, $A > 0$, $B > 0$ and $C > 0$, and we conclude that $\det(M) > 0$.

The system (2.5) has then a single solution $(\lambda_1, \mu_1, \lambda_2, \mu_2)^T$, leading to the existence and uniqueness of u_η solution of (2.2). $\square$

2.3. Convergence

We now investigate the limit of u_η when η goes to zero. We have the following result:

Lemma 2.3. *The solution u_η of the penalized problem* (2.2) *simply converges, when $\eta \to 0^+$, to $\bar{u}$ with*

- $\bar{u}_{|]0,1[} = u$ *solution of the original problem* (2.1),
- $\bar{u}_{|]1,2[} = v$ *solution of* $\begin{cases} v' + \alpha v = g(1) & \text{in }]1,2[\\ v(1) = u(1). \end{cases}$

In other words,

$$\lim_{\eta \to 0^+} u_\eta(x) = \begin{cases} u(x) & \text{if } x \in [0,1] \\ \dfrac{(\alpha u(1) - g(1))e^{\alpha}}{\alpha} e^{-\alpha x} + \dfrac{g(1)}{\alpha} & \text{if } x \in [1,2] \text{ and } \alpha > 0 \\ g(1)x + (u(1) - g(1)) & \text{if } x \in [1,2] \text{ and } \alpha = 0. \end{cases} \tag{2.6}$$

Proof. One has

$$\lim_{\eta\to 0^+} r_1 = +\infty \ \left(r_1 \sim \frac{1}{\eta}\right) \quad \text{and} \quad \lim_{\eta\to 0^+} r_2 = -\alpha.$$

Introducing $\lambda_2^* = \lambda_2 r_1 e^{2r_1}$ and $\mu_2^* = \mu_2 + \frac{g(1)}{\eta+\alpha}$, one has for $x \in [1,2]$,

$$u_\eta(x) = \lambda_2^* \frac{1}{r_1 e^{2r_1}} e^{r_1 x} + \mu_2^* e^{r_2 x} - \frac{g(1)}{\eta+\alpha} e^{r_2 x} + \frac{g(1)}{\eta+\alpha},$$

and

$$\begin{aligned}
\frac{1}{r_1 e^{2r_1}} e^{r_1 x} &= \frac{1}{r_1} e^{r_1(x-2)} \xrightarrow[\eta\to 0^+]{} 0, \\
\frac{g(1)}{\eta+\alpha} - \frac{g(1)}{\eta+\alpha} e^{r_2 x} &\xrightarrow[\eta\to 0^+]{} g(1)\frac{1-e^{-\alpha x}}{\alpha} && \text{if } \alpha > 0, \\
\frac{g(1)}{\eta+\alpha} - \frac{g(1)}{\eta+\alpha} e^{r_2 x} &= g(1)\frac{e^{r_2 x}-1}{r_2}\frac{r_2}{-\eta} \xrightarrow[\eta\to 0^+]{} g(1)x && \text{if } \alpha = 0.
\end{aligned}$$

Looking at the system satisfied by $(\lambda_1, \mu_1, \lambda_2^*, \mu_2^*)^T$, the system (2.5) reads now $A_\eta X_\eta = b_\eta$ as follows:

$$\begin{pmatrix} \alpha-1 & \alpha+1 & 0 & 0 \\ 0 & 0 & \frac{\alpha}{r_1}+1 & (\alpha+r_2)e^{2r_2} \\ e & e^{-1} & -\frac{1}{r_1 e^{r_1}} & -e^{r_2} \\ e & -e^{-1} & -\frac{1}{e^{r_1}} & -r_2 e^{r_2} \end{pmatrix} \begin{pmatrix} \lambda_1 \\ \mu_1 \\ \lambda_2^* \\ \mu_2^* \end{pmatrix} = \begin{pmatrix} 0 \\ g(1) - \alpha\frac{g(1)}{\eta+\alpha} + \frac{g(1)}{\eta+\alpha} r_2 e^{2r_2} + \alpha\frac{g(1)}{\eta+\alpha} e^{2r_2} \\ \frac{g(1)}{\eta+\alpha} - u(1) - \frac{g(1)}{\eta+\alpha} e^{r_2} \\ \alpha u(1) - g(1) - \frac{g(1)}{\eta+\alpha} r_2 e^{r_2} \end{pmatrix}. \tag{2.7}$$

The matrix A_η is invertible since $\det(A_\eta) = \frac{1}{r_1 e^{2r_1}} \det(M) \neq 0$. Moreover, $A_\eta \xrightarrow[\eta\to 0^+]{} A$ and $b_\eta \xrightarrow[\eta\to 0^+]{} b$ with

$$A = \begin{pmatrix} \alpha-1 & \alpha+1 & 0 & 0 \\ 0 & 0 & 1 & 0 \\ e & e^{-1} & 0 & -e^{-\alpha} \\ e & -e^{-1} & 0 & \alpha e^{-\alpha} \end{pmatrix}, \ b = \begin{pmatrix} 0 \\ 0 \\ \frac{g(1)}{\alpha} - u(1) - \frac{g(1)}{\alpha} e^{-\alpha} \\ \alpha u(1) - g(1) + g(1)e^{-\alpha} \end{pmatrix} \text{ if } \alpha > 0, \ b = \begin{pmatrix} 0 \\ 0 \\ g(1) - u(1) \\ 0 \end{pmatrix} \text{ if } \alpha = 0.$$

Since A is invertible, it follows that $X_\eta = A_\eta^{-1} b_\eta \xrightarrow[\eta\to 0^+]{} A^{-1} b = X$. We obtain

$$X = \begin{pmatrix} 0 \\ 0 \\ 0 \\ \frac{(\alpha u(1) - g(1) + g(1)e^{-\alpha})e^{\alpha}}{\alpha} \end{pmatrix} \text{ if } \alpha > 0 \qquad X = \begin{pmatrix} 0 \\ 0 \\ 0 \\ u(1) - g(1) \end{pmatrix} \text{ if } \alpha = 0.$$

Finally, taking the limit $\eta \to 0^+$ in (2.4) yields the desired result. $\square$

Remark 2.4. The positive sign in front of the penalization term in problem (2.2) is important: the penalized problem with the opposite sign has also a unique solution u_η for every $\eta > 0$ but this solution generally does not converge to the solution u of (2.1) in $[0,1]$. The sign determines the direction of advection $(\frac{\chi}{\eta} u'_\eta)$, the positive sign thus means a convection to the right: what happens in the domain $[1,2]$ does not influence the solution in $[0,1]$ when η approaches 0.

2.4. Error estimate

We have the following error estimate:

Lemma 2.5. *In the domain* $[0,1]$, $\|u_\eta - u\| = \underset{\eta\to 0^+}{O}(\eta)$ *for* L^∞, L^1, L^2 *and* H^1 *norms.*

Proof. Following (2.4), for $x \in [0,1]$, one has $u_\eta(x) - u(x) = \lambda_1 e^x + \mu_1 e^{-x}$ and $u'_\eta(x) - u'(x) = \lambda_1 e^x - \mu_1 e^{-x}$. In addition, $(\alpha-1)\lambda_1 + (\alpha+1)\mu_1 = 0$ from (2.7) and λ_1 is given using Cramer's rule by:

$$\lambda_1 = \frac{\det(A_{\eta\lambda_1})}{\det(A_\eta)} = \frac{\begin{vmatrix} 0 & \alpha+1 & 0 & 0 \\ g(1)\left(1+\frac{(r_2+\alpha)e^{2r_2}-\alpha}{\eta+\alpha}\right) & 0 & \frac{\alpha}{r_1}+1 & (\alpha+r_2)e^{2r_2} \\ g(1)\frac{1-e^{r_2}}{\eta+\alpha} - u(1) & e^{-1} & -\frac{1}{r_1 e^{r_1}} & -e^{r_2} \\ \alpha u(1) - g(1)\left(1+\frac{r_2 e^{r_2}}{\eta+\alpha}\right) & -e^{-1} & -\frac{1}{e^{r_1}} & -r_2 e^{r_2} \end{vmatrix}}{\det(A_\eta)}. \tag{2.8}$$

Using Taylor or asymptotic expansions as $\eta \to 0^+$, we obtain $\det(A_\eta) = \det(A) + o(1)$ and $\det(A_{\eta\lambda 1}) = -(\alpha+1)e^{-\alpha}(g(1)\alpha + u(1)(1-\alpha^2))\eta + o(\eta)$ in both cases $\alpha > 0$ and $\alpha = 0$.
Finally,

$$\lambda_1 = -\frac{(\alpha+1)(g(1)\alpha + u(1)(1-\alpha^2))}{(1+\alpha^2)(e-e^{-1}) + 2\alpha(e+e^{-1})}\eta + o(\eta) \quad \text{and} \quad \mu_1 = \frac{1-\alpha}{1+\alpha}\lambda_1.$$

Using the estimates $\lambda_1 = O(\eta)$ and $\mu_1 = O(\eta)$ as $\eta \to 0^+$, the result of Lemma 2.5 is now straightforward. □

2.5. Stability

The following result provides information about the continuous dependence of the solution u_η on the data f and g:

Lemma 2.6. *The application* $(f,g) \in L^2(]0,1[) \times L^2(\{0,1\}) \mapsto u_{\eta\,|]0,1[} \in H^1(]0,1[)$ *is linear continuous for all* $\eta > 0$. *In addition*

$$\exists C > 0, \quad \|u_\eta\|_{H^1(]0,1[)} \underset{\eta\to 0^+}{\leq} C(\|f\|_{L^2} + \|g\|_{L^2(\{0,1\})}),$$

where C *is independent of* η.

Proof. The linearity of the application is a consequence of the linearity of the penalized problem (2.2). Expanding the determinant at the numerator of (2.8) along the first column and using that the determinant at the denominator depends only on η (α being fixed), we can write $\lambda_1 = g(1)D^1_\eta + u(1)D^2_\eta$. Thus, using also $\mu_1 = \frac{1-\alpha}{1+\alpha}\lambda_1$,

$$\begin{aligned} \|u_\eta\|_{H^1(]0,1[)} &\leq |\lambda_1| \|e^x + \tfrac{1-\alpha}{1+\alpha}e^{-x}\|_{H^1(]0,1[)} + \|u\|_{H^1(]0,1[)} \\ &\leq C_1 D_\eta(|g(1)| + |u(1)|) + \|u\|_{H^1(]0,1[)}, \end{aligned} \tag{2.9}$$

where $D_\eta = \max(|D^1_\eta|, |D^2_\eta|)$.

On the other hand, the application $(f,g) \in L^2(]0,1[) \times L^2(\{0,1\}) \mapsto u \in H^1(]0,1[)$ is linear continuous. Indeed, taking as test function u itself in the weak formulation yields

$$\int_0^1 \left((u')^2 + u^2\right) dx + \alpha\big(u(0)^2 + u(1)^2\big) = \int_0^1 f u \, dx + \big(g(0)u(0) + g(1)u(1)\big),$$

and

$$\begin{aligned} \|u\|_{H^1}^2 &\leq \|f\|_{L^2}\|u\|_{L^2} + \|g\|_{L^2(\{0,1\})}\|u\|_{L^2(\{0,1\})} \\ &\leq \|f\|_{L^2}\|u\|_{H^1} + C_2\|g\|_{L^2(\{0,1\})}\|u\|_{H^1} \end{aligned}$$

using the continuity of the trace application. Hence $\|u\|_{H^1} \leq C_3(\|f\|_{L^2} + \|g\|_{L^2(\{0,1\})})$, where $C_3 = \max(1, C_2)$.

Using also $|g(1)| \leq \sqrt{g^2(0) + g^2(1)} \leq \|g\|_{L^2(\{0,1\})}$ and $|u(1)| \leq \sqrt{u^2(0) + u^2(1)} \leq \|u\|_{L^2(\{0,1\})} \leq C_2\|u\|_{H^1}$, (2.9) gives $\|u_\eta\|_{H^1(]0,1[)} \leq C_\eta(\|f\|_{L^2} + \|g\|_{L^2(\{0,1\})})$, where $C_\eta = C_1 D_\eta(1 + C_2 C_3) + C_3$, which proves the continuity of the considered linear application for all $\eta > 0$.

By reconsidering the expansion of the determinant $\det(A_{\eta\lambda_1})$ along the first column, we find using the Taylor expansion obtained for λ_1 as $\eta \to 0^+$ in the proof of Lemma 2.5 that $D_\eta^1 = -\frac{(\alpha+1)\alpha}{(1+\alpha^2)(e-e^{-1})+2\alpha(e+e^{-1})}\eta + o(\eta)$ and $D_\eta^2 = -\frac{(\alpha+1)(1-\alpha^2)}{(1+\alpha^2)(e-e^{-1})+2\alpha(e+e^{-1})}\eta + o(\eta)$. Therefore $D_\eta \xrightarrow[\eta \to 0^+]{} 0$ and $C_\eta \xrightarrow[\eta \to 0^+]{} C_3$, the continuity constant of the original problem. We thus obtain finally the inequality

$$\|u_\eta\|_{H^1(]0,1[)} \underset{\eta \to 0^+}{\leq} C(\|f\|_{L^2} + \|g\|_{L^2(\{0,1\})})$$

for a constant $C = C_3 + \varepsilon$ independent of η. $\square$

2.6. Numerical approximation

For the numerical approximation, we consider the geometry that arises in plasma application: the fluid domain where the initial equation is raised is $\omega =]0, x_l[\cup]x_r, 1[$ and the solid obstacle is located in $]x_l, x_r[$ centered at $x = 0.5$, with $x_l = 0.5(1-d)$ and $x_r = 0.5(1+d)$ where d is the size of the obstacle, as represented in Figure 1 right. The reaction-diffusion equation is satisfied in ω with Robin boundary conditions at the obstacle boundary $\{x_l, x_r\}$ and periodic boundary conditions at $x = 0$ and $x = 1$, corresponding to the physical situation. Therefore, the initial problem reads

$$\begin{cases} -u'' + u = f \quad \text{in }]0, x_l[\cup]x_r, 1[\\ u'(x_l) + \alpha u(x_l) = g(x_l), \ -u'(x_r) + \alpha u(x_r) = g(x_r) \\ u(0) = u(1), \ u'(0) = u'(1). \end{cases} \tag{2.10}$$

The penalization technique proposed in the previous sections applies here as follows:

$$\begin{cases} -u_\eta'' + u_\eta + \dfrac{\chi_l}{\eta}\big(u_\eta' + \alpha u_\eta - g(x_l)\big) + \dfrac{\chi_r}{\eta}\big(-u_\eta' + \alpha u_\eta - g(x_r)\big) = (1-\chi)f \quad \text{in }]0,1[\\ u_\eta(0) = u_\eta(1), \ u_\eta'(0) = u_\eta'(1), \end{cases} \tag{2.11}$$

where χ is the characteristic function of the entire obstacle domain $]x_l, x_r[$, χ_l is the characteristic function of the left part $]x_l, x_l + \Delta_l[$ of the obstacle domain and χ_r is the characteristic function of the right part $]x_r - \Delta_r, x_r[$. Δ_l and Δ_r satisfy $\Delta_l + \Delta_r < d = x_r - x_l$ ensuring that both intervals are disjoint, see Figure 1 right.

Adapting the theoretical results obtained for the problem (2.1) and its penalization (2.2), it can be shown that the penalized problem (2.11) is well-posed in its weak form for all $\eta > 0$, and that its unique solution u_η tends, when η goes to 0, to a function $\bar{u}$ whose restriction to $]0, x_l[\cup]x_r, 1[$ is the solution u of the original problem (2.10).

Remark 2.7. As in Remark 2.4, the signs considered in (2.11) for the penalization terms were chosen in order to have an advection which goes from the fluid domain to the solid domain. In addition, a free part was introduced in the middle of the obstacle to avoid communication between left and right parts when η goes to 0.

2.6.1. Numerical analysis

The penalized problem (2.11) is discretized using finite differences. We consider a uniform subdivision $(x_i)_{1\le i\le N+1}$ of $[0,1]$ of step size h ($x_i = (i-1)h = \frac{i-1}{N}$) and the following scheme:

$$\begin{cases} -\dfrac{U_{i+1} - 2U_i + U_{i-1}}{h^2} + U_i + \dfrac{\chi_l(x_i)}{\eta}\Big(\dfrac{U_i - U_{i-1}}{h} + \alpha U_i - g_l\Big) \\ \quad + \dfrac{\chi_r(x_i)}{\eta}\Big(-\dfrac{U_{i+1} - U_i}{h} + \alpha U_i - g_r\Big) = (1 - \chi(x_i))f(x_i) \quad i = 1, \dots, N \\ U_0 = U_N, \ U_1 = U_{N+1}. \end{cases} \tag{2.12}$$

To simplify the notations, we use g_l instead of $g(x_l)$ and g_r instead of $g(x_r)$. The vector $(U_i)_{1\le i\le N+1}$ is expected to be an approximation of $(u_\eta(x_i))_{1\le i\le N+1}$. The linear system $A_h U_h = r_h$ associated with (2.12) reads

$$\begin{pmatrix} b_1 & c_1 & 0 & \cdots & 0 & a_1 \\ a_2 & b_2 & c_2 & \ddots & \ddots & 0 \\ 0 & \ddots & \ddots & \ddots & \ddots & \vdots \\ \vdots & \ddots & \ddots & \ddots & \ddots & 0 \\ 0 & \ddots & \ddots & a_{N-1} & b_{N-1} & c_{N-1} \\ c_N & 0 & \cdots & 0 & a_N & b_N \end{pmatrix} \begin{pmatrix} U_1 \\ U_2 \\ \vdots \\ \vdots \\ U_{N-1} \\ U_N \end{pmatrix} = \begin{pmatrix} r_1 \\ r_2 \\ \vdots \\ \vdots \\ r_{N-1} \\ r_N \end{pmatrix}, \tag{2.13}$$

where $a_i = -\frac{1}{h^2} - \frac{\chi_l(x_i)}{\eta}\frac{1}{h}$, $b_i = 1 + \frac{2}{h^2} + \frac{\chi_l(x_i)+\chi_r(x_i)}{\eta}(\frac{1}{h} + \alpha)$, $c_i = -\frac{1}{h^2} - \frac{\chi_r(x_i)}{\eta}\frac{1}{h}$ and $r_i = (1 - \chi(x_i))f(x_i) + \frac{\chi_l(x_i)}{\eta}g_l + \frac{\chi_r(x_i)}{\eta}g_r$. We prove in the following the consistency and the stability of the finite difference scheme.

Lemma 2.8 (Existence and uniqueness)**.** *For all $\eta, h > 0$, the system* (2.13) *has a unique solution.*

Proof. For $1 \le i \le N$, one has $b_i > 0$, $a_i < 0$ and $c_i < 0$, thus

$$\begin{aligned} |b_i| = b_i = 1 - a_i - c_i + \tfrac{\chi_l(x_i)+\chi_r(x_i)}{\eta}\alpha &= 1 + |a_i| + |c_i| + \tfrac{\chi_l(x_i)+\chi_r(x_i)}{\eta}\alpha \\ &\ge 1 + |a_i| + |c_i| > |a_i| + |c_i|. \end{aligned}$$

A_h is consequently a strictly diagonally dominant matrix, hence invertible by the Hadamard lemma. $\square$

Lemma 2.9 (Stability)**.** *For all $\eta, h > 0$, the finite difference scheme* (2.13) *is stable in the norm $\|\cdot\|_\infty$ with $\|A_h^{-1}\|_\infty \leq 1$.*

Proof. The main argument is that the matrix A_h is strictly diagonally dominant with $\left|(A_h)_{ii}\right| - \sum_{j\neq i}\left|(A_h)_{ij}\right| \geq \delta > 0$ where δ is independent of h.

Considering $M \in \{1, \ldots, N\}$ such that $|U_M| = \max_{1\leq i\leq N} |U_i| = \|U_h\|_\infty$, it follows

$$|r_M| = \begin{cases} |b_1U_1 + c_1U_2 + a_1U_N| \geq |b_1U_1| - |a_1U_N| - |c_1U_2| & \text{if } M = 1 \\ |a_MU_{M-1} + b_MU_M + c_MU_{M+1}| \geq |b_MU_M| - |a_MU_{M-1}| - |c_MU_{M+1}| & \text{if } 2 \leq M \leq N-1 \\ |c_NU_1 + a_NU_{N-1} + b_NU_N| \geq |b_NU_N| - |a_NU_{N-1}| - |c_NU_1| & \text{if } M = N, \end{cases}$$

which shows that in all cases $|U_M| \leq |r_M|$ since $|b_M| - |a_M| - |c_M| \geq 1$ and $-|U_i| \geq -|U_M|$. Finally, using $|r_M| \leq \|r_h\|_\infty$ we obtain $\|U_h\|_\infty \leq \|r_h\|_\infty$ that is $\|A_h^{-1}\|_\infty \leq 1$. □

Lemma 2.10 (Consistency)**.** *For all $\eta > 0$, if the solution u_η of* (2.11) *satisfies $u_\eta \in C^3(\mathbb{R})$ then the scheme* (2.13) *is first-order consistent with*

$$\|\varepsilon_h\|_\infty = \|A_h\mathcal{U}_h - r_h\|_\infty \leq h\Big(\frac{1}{\eta}\max_{0\leq x\leq 1}|u''_\eta(x)| + \frac{1}{3}\max_{0\leq x\leq 1}|u^{(3)}_\eta(x)|\Big),$$

where $\mathcal{U}_h = (u_\eta(x_1), \ldots, u_\eta(x_N))^T$.

Proof. For $u_\eta \in C^3$, straightforward Taylor-Lagrange formula gives the desired result. □

Theorem 2.11 (Convergence)**.** *For all $\eta > 0$, if the solution u_η of* (2.11) *satisfies $u_\eta \in C^3(\mathbb{R})$ then the scheme* (2.13) *is first-order convergent in the norm $\|\cdot\|_\infty$ with*

$$\|e_h\|_\infty = \|\mathcal{U}_h - U_h\|_\infty \leq C_\eta h,$$

where $\mathcal{U}_h = (u_\eta(x_1), \ldots, u_\eta(x_N))^T$ and C_η is a constant independent of h.

Proof. Convergence is a consequence of the Lax theorem: the finite difference scheme (2.13) is stable (Lemma 2.9) and consistent (Lemma 2.10). □

2.6.2. Numerical tests

In this section, numerical experiments are performed to validate the approximation of the solution of the original problem (2.10) by the numerical solution of the penalized problem (2.11) discretized with the first-order finite difference scheme (2.12). We also present the results obtained using the following second-order finite difference scheme:

$$\begin{cases} -\dfrac{U_{i+1} - 2U_i + U_{i-1}}{h^2} + U_i + \dfrac{\chi_l(x_i)}{\eta}\Big(\dfrac{3U_i - 4U_{i-1} + U_{i-2}}{2h} + \alpha U_i - g_l\Big) \\ \quad + \dfrac{\chi_r(x_i)}{\eta}\Big(-\dfrac{-U_{i+2} + 4U_{i+1} - 3U_i}{2h} + \alpha U_i - g_r\Big) = (1 - \chi(x_i))f(x_i) \quad i = 1, \ldots, N \\ U_i = U_{N+i}, \end{cases} \tag{2.14}$$

involving a cyclic pentadiagonal matrix.

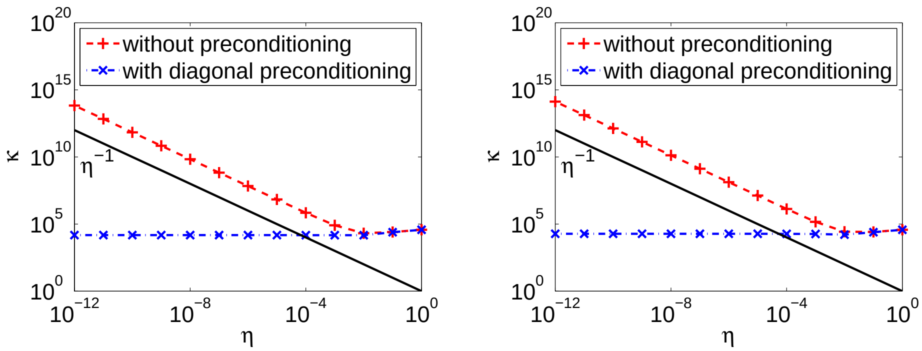

(a) First-order scheme (2.12) (b) Second-order scheme (2.14)

Figure 2: Condition number $\kappa(A_h)$ in the 2-norm of the matrix of the finite difference scheme versus the penalization parameter η for $\alpha = 1$, $d = 0.1$, $\Delta_l = \Delta_r = 0.3d$ and $h = 10^{-2}$.

For both considered schemes, (2.12) and (2.14), the penalization introduces terms of order η^{-1} in the matrix A_h, which leads to an ill-conditioned matrix problem for small values of the penalization parameter η. As shown in Figure 2, for a fixed space step h, the condition number $\kappa(A_h) = \|A_h\| \cdot \|A_h^{-1}\|$ (in the 2-norm defined in ℓ^2) varies linearly with respect to η^{-1} for $\eta \ll 1$. However, applying a diagonal preconditioner, $C = \mathrm{diag}(A_h)$, allows to obtain a condition number almost independent of η as shown in Figure 2. This preconditioning does not resolve the poor conditioning associated with the second-order derivative that induces a resulting conditioning $\kappa(C^{-1}A_h) = O(h^{-2})$. However, one could make the condition number independent of h using a conventional preconditioner suitable for elliptic operators.

The numerical solutions of the penalized problem (2.11) using the finite difference schemes (2.12) and (2.14) are compared to the exact solution of the problem (2.10) for different types of conditions:

1. Nonhomogeneous Neumann boundary conditions ($u'(x_l) = 1$, $u'(x_r) = 2$) in Figure 3;
2. Robin boundary conditions ($u'(x_l) + u(x_l) = 0$, $-u'(x_r) + u(x_r) = 0$) in Figure 4.

We chose $d = 0.1$ (i.e. $x_l = 0.45$ and $x_r = 0.55$ for the obstacle boundary) and $\Delta_l = \Delta_r = 0.3d$. The different masks are $\chi = \chi_{[x_l,x_r]}$, $\chi_l = \chi_{[x_l,x_l+\Delta_l]}$ and $\chi_r = \chi_{[x_r-\Delta_r,x_r]}$ (all intervals were taken closed to ensure in particular $\chi(x_l) = \chi_l(x_l)$ and $\chi(x_r) = \chi_r(x_r)$).

The errors represented on Figures 3(c), 3(d), 4(c) and 4(d) correspond to $\|\mathcal{V}_h - U_h\|$ inside the fluid domain ω, where $\mathcal{V}_h = (u(x_1), \ldots, u(x_N))^T$. For a fixed norm, we write $\|\mathcal{V}_h - U_h\| \le \|\mathcal{V}_h - \mathcal{U}_h\| + \|\mathcal{U}_h - U_h\|$, where $\|\mathcal{V}_h - \mathcal{U}_h\|$ is an error related to the penalization method and provides information on the effect of the parameter η, and $\|\mathcal{U}_h - U_h\|$ is an error introduced by the spatial discretization.

Based on the theoretical estimates obtained previously, the following bound $\|\mathcal{V}_h - U_h\|_\infty \le C\eta + C_\eta h^p$, where $p = 1$ for the first-order scheme (2.12) and $p = 2$ for the second-order scheme (2.14) is expected.

Provided that η is small enough leading to a negligible penalization error, the error measured as a function of h (Figures 3(c) and 4(c)) gives an order of convergence consistent with the chosen discretizations.

Similarly, provided that h is small enough to neglect the discretization error, the error measured with respect to η allows to evaluate the order of convergence of u_η to u in the fluid

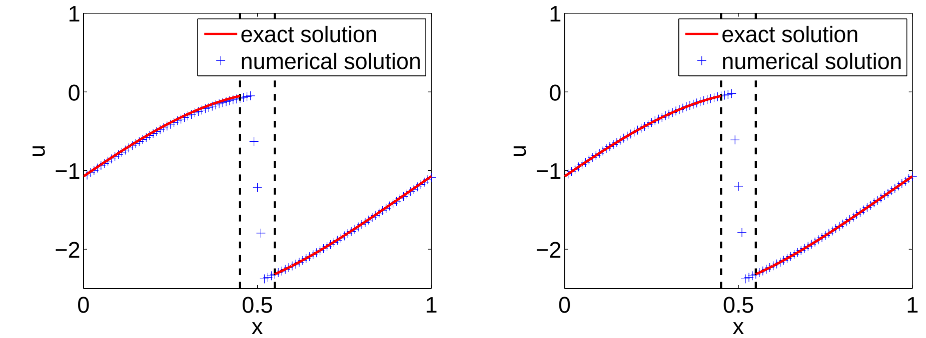

(a) First-order scheme (2.12) (b) Second-order scheme (2.14)

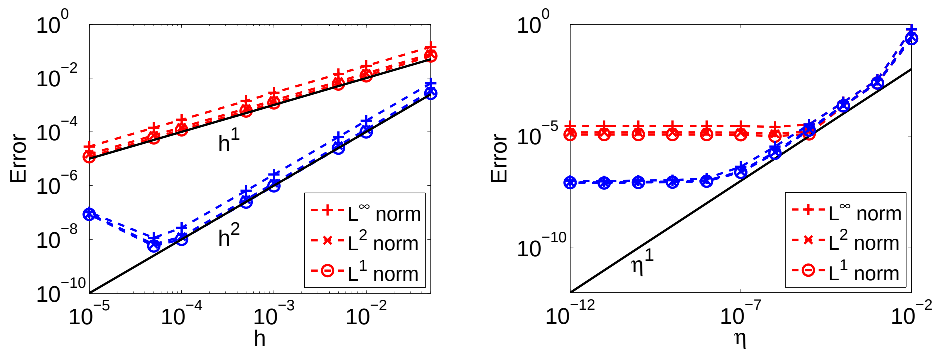

(c) $\eta = 10^{-10}$ (d) $h = 10^{-5}$

Figure 3: Comparison between the numerical solution of the penalized elliptic problem (2.11) and the exact solution of the original problem (2.10) with nonhomogeneous Neumann boundary conditions. (a)-(b): $\eta = 10^{-10}$ and $h = 10^{-2}$. Errors versus h (c) and errors versus η (d) for first (red) and second (blue) order schemes.

domain. The errors obtained for $h = 10^{-5}$ in Figures 3(d) and 4(d) show a linear decrease when $\eta \to 0$, as obtained theoretically in Lemma 2.5, thus revealing the effective control of the penalization parameter over the boundary conditions.

3. Parabolic equation

In this section, we consider the following parabolic equation with Robin boundary conditions:

$$\begin{cases} \dfrac{\partial u}{\partial t} - \Delta u = f & \text{in } \omega \times]0, T[\\ \dfrac{\partial u}{\partial n} + \alpha u = g & \text{on } \partial\omega \times]0, T[\\ u(x, 0) = u_0(x) & \text{in } \omega, \end{cases} \tag{3.1}$$

where ω is a given smooth bounded open set in $\mathbb{R}^D$, n is the outward-pointing unit normal vector on the boundary $\partial\omega$, u_0 is the initial condition, f and g are source terms, and $\alpha \geq 0$.

We first recall some results concerning the solution of this problem and its time discretization. Then the penalization method is introduced and analyzed and numerical examples are given.

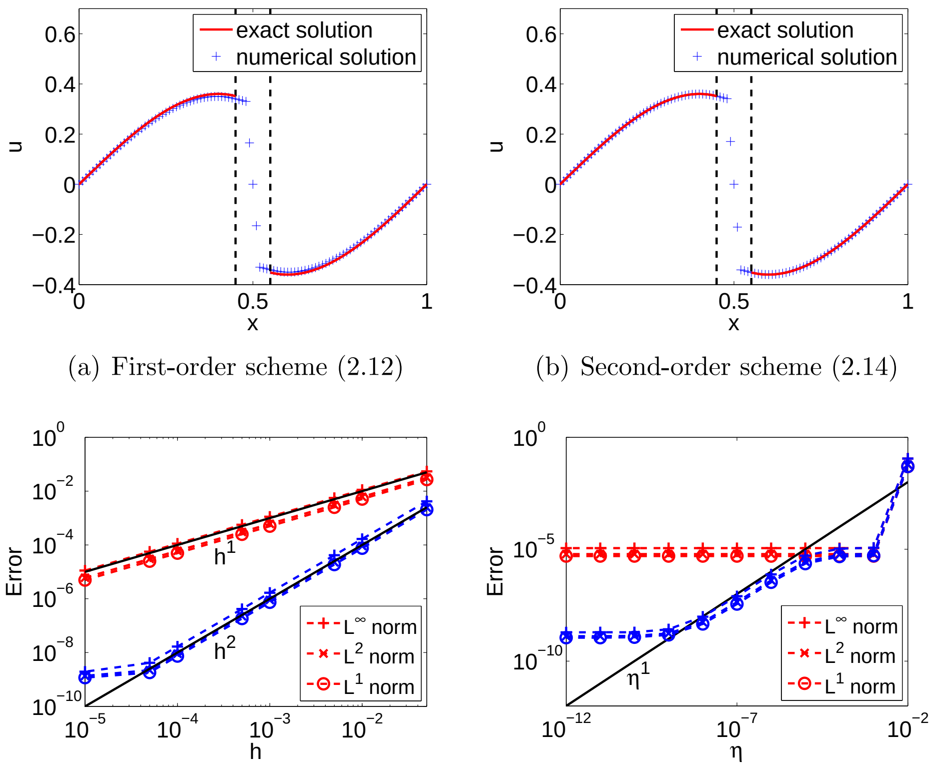

(a) First-order scheme (2.12)

(b) Second-order scheme (2.14)

(c) $\eta = 10^{-10}$

(d) $h = 10^{-5}$

Figure 4: Comparison between the numerical solution of the penalized elliptic problem (2.11) and the exact solution of the original problem (2.10) with Robin boundary conditions. (a)-(b): $\eta = 10^{-10}$ and $h = 10^{-2}$. Errors versus h (c) and errors versus η (d) for first (red) and second (blue) order schemes.

3.1. Preliminaries

3.1.1. Existence and uniqueness

Existence and uniqueness can be proved using the classical Fourier or diagonalization method [12, 1]. We have the following lemma (see Appendix A for the details of the proof):

Lemma 3.1. *The heat equation with Robin boundary conditions* (3.1) *where* $u_0 \in L^2(\omega)$*,* $f \in L^2(]0,T[; L^2(\omega))$ *and* $g \in C^1([0,T]; H^{1/2}(\partial\omega))$ *admits a unique solution* $u \in L^2(]0,T[; H^1(\omega)) \cap C([0,T]; L^2(\omega))$.

3.1.2. Time discretization

Assuming that the data are smooth ($f \in C(\bar{\omega} \times [0,T])$ and $g \in C^1(\partial\omega \times [0,T])$), we discretize in time the problem (3.1) using the implicit Euler scheme (for sake of simplicity):

$$\begin{cases} \dfrac{u^{n+1} - u^n}{\Delta t} - \Delta u^{n+1} = f(t^{n+1}) & \text{in } \omega \\ \dfrac{\partial u^{n+1}}{\partial n} + \alpha u^{n+1} = g(t^{n+1}) & \text{on } \partial\omega \\ u^0 = u_0, & \end{cases} \tag{3.2}$$

where $\Delta t = \frac{T}{M}$ $(M \in \mathbb{N}^*)$ is the time step and $t^n = n\Delta t$ for $0 \leq n \leq M$. We consider the following weak formulation of (3.2):

$$\left| \begin{array}{l} \text{Find } u^{n+1} \in H^1(\omega) \text{ such that } \forall v \in H^1(\omega) \\ \langle u^{n+1}, v\rangle_{L^2(\omega)} + \Delta t\, a(u^{n+1}, v) = \langle u^n + \Delta t f(t^{n+1}), v\rangle_{L^2(\omega)} + \Delta t \displaystyle\int_{\partial\omega} g(t^{n+1}) v \, d\sigma, \end{array} \right. \tag{3.3}$$

where

$$\forall u, v \in H^1(\omega), \quad a(u,v) = \int_\omega \nabla u \cdot \nabla v \, dx + \alpha \int_{\partial\omega} uv \, d\sigma, \tag{3.4a}$$

$$\forall u, v \in L^2(\omega), \quad \langle u, v\rangle_{L^2(\omega)} = \int_\omega uv \, dx. \tag{3.4b}$$

Using the Lax-Milgram theorem, the sequence $(u^n)_{0\leq n\leq M}$ is uniquely defined and $u^n \in H^1(\omega)$ for $n \geq 1$.

A direct adaption of the proof in [7, Part I] for Dirichlet boundary conditions allows to handle Robin boundary conditions and to obtain the following result:

Lemma 3.2. *If the solution u of (3.1) satisfies $u \in C^2(\bar{\omega}\times[0,T])$ then the time discretization (3.2) is first-order convergent in the norm $\|\cdot\|_{L^2}$ with*

$$\sup_{0\leq n\leq M} \|e^n\|_{L^2} = \sup_{0\leq n\leq M} \|u(t^n) - u^n\|_{L^2} \leq \Delta t \frac{T\sqrt{|\omega|}}{2} \|u\|_{C^2}.$$

3.2. Penalization

We present here the penalization method proposed for the heat equation with Robin boundary conditions (3.1) in the spatial univariate case ($D = 1$) with the geometry of Figure 1 left. In this case, the problem is written

$$\begin{cases} \dfrac{\partial u}{\partial t} - \dfrac{\partial^2 u}{\partial x^2} = f & x \in]0,1[,\ t \in]0,T[\\ -\dfrac{\partial u}{\partial x}(0,t) + \alpha u(0,t) = g(0,t) & t \in]0,T[\\ \dfrac{\partial u}{\partial x}(1,t) + \alpha u(1,t) = g(1,t) & t \in]0,T[\\ u(x,0) = u_0(x) & x \in]0,1[. \end{cases} \tag{3.5}$$

Time discretization (3.2) and penalization of the resulting sequence of elliptic problems lead to

$$\begin{cases} -u_\eta^{n+1\prime\prime} + \dfrac{1}{\Delta t} u_\eta^{n+1} + \dfrac{\chi}{\eta}\big(u_\eta^{n+1\prime} + \alpha u_\eta^{n+1} - g(1, t^{n+1})\big) \\ \qquad\qquad\qquad\qquad = (1-\chi)\Big(f(t^{n+1}) + \dfrac{1}{\Delta t} u_\eta^n\Big) \quad \text{in }]0,2[\\ -u_\eta^{n+1\prime}(0) + \alpha u_\eta^{n+1}(0) = g(0, t^{n+1}),\ \ u_\eta^{n+1\prime}(2) + \alpha u_\eta^{n+1}(2) = g(1, t^{n+1}) \\ u_\eta^0 = (1-\chi) u_0, \end{cases} \tag{3.6}$$

where again $\eta > 0$ is the penalization parameter and χ is the characteristic function of the domain $]1,2[$. Using Lemma 2.2 (which remains valid with nonunit coefficients), the sequence $(u_\eta^n)_{0\le n\le M}$ is uniquely defined and $u_\eta^n \in C^1([0,2])$ for $n \geq 1$. The influence of parameter η is presented in the following lemma:

Lemma 3.3. *For all $\Delta t > 0$,*

$$\sup_{0\le n\le M} \|u_\eta^n - u^n\|_{H^1(]0,1[)} \underset{\eta\to 0^+}{\leq} C_{\Delta t}\,\eta, \tag{3.7}$$

where $C_{\Delta t}$ is a constant independent of η.

Proof. Let $\Delta t > 0$ be fixed. We will show by induction on n that

$$\forall 0 \le n \le M, \quad \|u_\eta^n - u^n\|_{H^1(]0,1[)} \underset{\eta\to 0^+}{\leq} C_{n,\Delta t}\,\eta.$$

As $u_\eta^0 = u_0 = u^0$ in $]0,1[$, the result holds for $n = 0$. Assume that $\|u_\eta^n - u^n\|_{H^1(]0,1[)} \underset{\eta\to 0^+}{\leq} C_{n,\Delta t}\,\eta$ for some integer $n \geq 0$. Considering v_η^{n+1} solution of

$$\begin{cases} -v_\eta^{n+1\,\prime\prime} + \dfrac{1}{\Delta t} v_\eta^{n+1} + \dfrac{\chi}{\eta}\big(v_\eta^{n+1\,\prime} + \alpha v_\eta^{n+1} - g(1,t^{n+1})\big) \\ \qquad\qquad\qquad\qquad = (1-\chi)\Big(f(t^{n+1}) + \dfrac{1}{\Delta t} u^n\Big) \quad \text{in }]0,2[\\ -v_\eta^{n+1\,\prime}(0) + \alpha v_\eta^{n+1}(0) = g(0,t^{n+1}),\ v_\eta^{n+1\,\prime}(2) + \alpha v_\eta^{n+1}(2) = g(1,t^{n+1}), \end{cases}$$

one has $\|v_\eta^{n+1} - u^{n+1}\|_{H^1(]0,1[)} \underset{\eta\to 0^+}{\leq} C'_{n,\Delta t}\,\eta$ using Lemma 2.5 (which remains valid with nonunit coefficients). Introducing $w_\eta^{n+1} = u_\eta^{n+1} - v_\eta^{n+1}$, w_η^{n+1} satisfies

$$\begin{cases} -w_\eta^{n+1\,\prime\prime} + \dfrac{1}{\Delta t} w_\eta^{n+1} + \dfrac{\chi}{\eta}\big(w_\eta^{n+1\,\prime} + \alpha w_\eta^{n+1}\big) = (1-\chi)\Big(\dfrac{1}{\Delta t}(u_\eta^n - u^n)\Big) \quad \text{in }]0,2[\\ -w_\eta^{n+1\,\prime}(0) + \alpha w_\eta^{n+1}(0) = 0,\ w_\eta^{n+1\,\prime}(2) + \alpha w_\eta^{n+1}(2) = 0. \end{cases}$$

As in the proof of Lemma 2.6, we obtain a continuous dependence result for the solution w_η^{n+1} with respect to the data in $]0,1[$:

$$\begin{aligned} \|w_\eta^{n+1}\|_{H^1(]0,1[)} \underset{\eta\to 0^+}{\leq} C''_{\Delta t}\Big\|\frac{1}{\Delta t}(u_\eta^n - u^n)\Big\|_{L^2(]0,1[)} &\underset{\eta\to 0^+}{\leq} C'''_{\Delta t}\|u_\eta^n - u^n\|_{H^1(]0,1[)} \\ &\underset{\eta\to 0^+}{\leq} C'''_{\Delta t} C_{n,\Delta t}\,\eta, \end{aligned}$$

by the inductive hypothesis. It follows

$$\begin{aligned} \|u_\eta^{n+1} - u^{n+1}\|_{H^1(]0,1[)} &\leq \|u_\eta^{n+1} - v_\eta^{n+1}\|_{H^1(]0,1[)} + \|v_\eta^{n+1} - u^{n+1}\|_{H^1(]0,1[)} \\ &\underset{\eta\to 0^+}{\leq} (C'''_{\Delta t} C_{n,\Delta t} + C'_{n,\Delta t})\eta, \end{aligned}$$

which yields

$$\|u_\eta^{n+1} - u^{n+1}\|_{H^1(]0,1[)} \underset{\eta\to 0^+}{\leq} C_{n+1,\Delta t}\,\eta.$$

Finally, we obtain the result (3.7) by taking $C_{\Delta t} = \sup_{0\le n\le M} C_{n,\Delta t}$. $\square$

3.3. Numerical approximation

As for the numerical approximation of the elliptic case, the numerical tests are performed in the geometry of Figure 1 right. The problem then reads

$$\begin{cases} \dfrac{\partial u}{\partial t} - \dfrac{\partial^2 u}{\partial x^2} = f & x \in]0, x_l[\cup]x_r, 1[,\ t \in]0, T[\\ \dfrac{\partial u}{\partial x}(x_l, t) + \alpha u(x_l, t) = g(x_l, t) & t \in]0, T[\\ -\dfrac{\partial u}{\partial x}(x_r, t) + \alpha u(x_r, t) = g(x_r, t) & t \in]0, T[\\ u(0, t) = u(1, t),\ \dfrac{\partial u}{\partial x}(0, t) = \dfrac{\partial u}{\partial x}(1, t) & t \in]0, T[\\ u(x, 0) = u_0(x) & x \in]0, x_l[\cup]x_r, 1[. \end{cases} \tag{3.8}$$

We first perform the time discretization using the implicit Euler scheme, and the penalization method is then applied to the sequence of elliptic problems. We obtain:

$$\begin{cases} -u_\eta^{n+1\prime\prime} + \dfrac{1}{\Delta t} u_\eta^{n+1} + \dfrac{\chi_l}{\eta}\big(u_\eta^{n+1\prime} + \alpha u_\eta^{n+1} - g(x_l, t^{n+1})\big) \\ \qquad + \dfrac{\chi_r}{\eta}\big(-u_\eta^{n+1\prime} + \alpha u_\eta^{n+1} - g(x_r, t^{n+1})\big) = (1-\chi)\Big(f(t^{n+1}) + \dfrac{1}{\Delta t} u_\eta^n\Big) \quad \text{in }]0,1[\\ u_\eta^{n+1}(0) = u_\eta^{n+1}(1),\ u_\eta^{n+1\prime}(0) = u_\eta^{n+1\prime}(1) \\ u_\eta^0 = (1-\chi) u_0. \end{cases} \tag{3.9}$$

The last step consists of the spatial discretization.

3.3.1. Spatial discretization

As in Section 2.6.1, we consider a uniform subdivision $(x_i)_{1 \le i \le N+1}$ of $[0, 1]$ of space step h and introduce the following finite difference scheme:

$$\begin{cases} -\dfrac{U_{i+1}^{n+1} - 2U_i^{n+1} + U_{i-1}^{n+1}}{h^2} + \dfrac{U_i^{n+1}}{\Delta t} + \dfrac{\chi_l(x_i)}{\eta}\Big(\dfrac{U_i^{n+1} - U_{i-1}^{n+1}}{h} + \alpha U_i^{n+1} - g_l^{n+1}\Big) \\ \qquad + \dfrac{\chi_r(x_i)}{\eta}\Big(-\dfrac{U_{i+1}^{n+1} - U_i^{n+1}}{h} + \alpha U_i^{n+1} - g_r^{n+1}\Big) = (1 - \chi(x_i))\Big(f(x_i, t^{n+1}) + \dfrac{U_i^n}{\Delta t}\Big) \\ U_0^{n+1} = U_N^{n+1},\ U_1^{n+1} = U_{N+1}^{n+1} \\ U_i^0 = (1 - \chi(x_i)) u_0(x_i), \end{cases} \tag{3.10}$$

for $i = 1, \dots, N$ and $n = 0, \dots, M-1$. We note g_l^{n+1} resp. g_r^{n+1} for $g(x_l, t^{n+1})$ resp. $g(x_r, t^{n+1})$.

At each time step, this scheme leads to the resolution of the following linear system

$A_hU_h^{n+1} = B_hU_h^n + C_h^n$:

$$\begin{pmatrix} b_1 & c_1 & 0 & \cdots & 0 & a_1 \\ a_2 & b_2 & c_2 & \ddots & \ddots & 0 \\ 0 & \ddots & \ddots & \ddots & \ddots & \vdots \\ \vdots & \ddots & \ddots & \ddots & \ddots & 0 \\ 0 & \ddots & \ddots & a_{N-1} & b_{N-1} & c_{N-1} \\ c_N & 0 & \cdots & 0 & a_N & b_N \end{pmatrix} \begin{pmatrix} U_1^{n+1} \\ U_2^{n+1} \\ \vdots \\ \vdots \\ U_{N-1}^{n+1} \\ U_N^{n+1} \end{pmatrix} = \begin{pmatrix} r_1^n \\ r_2^n \\ \vdots \\ \vdots \\ r_{N-1}^n \\ r_N^n \end{pmatrix}, \tag{3.11}$$

where $a_i = -\frac{\Delta t}{h^2} - \frac{\chi_l(x_i)}{\eta}\frac{\Delta t}{h}$, $b_i = 1 + \frac{2\Delta t}{h^2} + \Delta t\frac{\chi_l(x_i)+\chi_r(x_i)}{\eta}(\frac{1}{h} + \alpha)$, $c_i = -\frac{\Delta t}{h^2} - \frac{\chi_r(x_i)}{\eta}\frac{\Delta t}{h}$ and $r_i^n = (1 - \chi(x_i))(\Delta t f(x_i, t^{n+1}) + U_i^n) + \Delta t\frac{\chi_l(x_i)}{\eta}g_l^{n+1} + \Delta t\frac{\chi_r(x_i)}{\eta}g_r^{n+1}$.

Theorem 3.4. *For all $\Delta t, \eta > 0$, if the solution u_η^n of (3.9) satisfies $u_\eta^n \in C^3(\mathbb{R})$ for all $0 \le n \le M$ then the space discretization (3.10) is first-order convergent in the norm $\|\cdot\|_\infty$ with*

$$\sup_{0\le n\le M} \|\mathcal{U}_h^n - U_h^n\|_\infty \le C_{\Delta t,\eta}\, h, \tag{3.12}$$

where $\mathcal{U}_h^n = (u_\eta^n(x_1), \ldots, u_\eta^n(x_N))^T$ and $C_{\Delta t,\eta}$ is a constant independent of h.

Proof. Defining the consistency error at time $n+1$ as:

$$\varepsilon_h^{n+1} = \frac{1}{\Delta t}(A_h\mathcal{U}_h^{n+1} - B_h\mathcal{U}_h^n - C_h^n),$$

we get, proceeding as in the elliptic case (see Lemma 2.10),

$$\begin{aligned} \|\varepsilon_h^{n+1}\|_\infty &\le h\Big(\frac{1}{\eta}\max_{0\le x\le 1}|u_\eta^{n+1\prime\prime}(x)| + \frac{1}{3}\max_{0\le x\le 1}|u_\eta^{n+1(3)}(x)|\Big) \\ &\le C_{n+1,\Delta t,\eta}\, h. \end{aligned}$$

One has $A_he_h^{n+1} = B_he_h^n + \Delta t\,\varepsilon_h^{n+1}$ where $e_h^n = \mathcal{U}_h^n - U_h^n$. As for the elliptic case, we obtain the invertibility and the stability of A_h in the $\|\cdot\|_\infty$ norm: $\|A_h^{-1}\|_\infty \le 1$ (see Lemmas 2.8 and 2.9). One also has $\|B_h\|_\infty \le 1$. Therefore,

$$\|e_h^{n+1}\|_\infty \le \|e_h^n\|_\infty + \Delta t\|\varepsilon_h^{n+1}\|_\infty,$$

thus for all $0 \le n \le M-1$,

$$\|e_h^{n+1}\|_\infty = \sum_{k=0}^{n}\|e_h^{k+1} - e_h^k\|_\infty \le \sum_{k=0}^{n}\Delta t\|\varepsilon_h^{k+1}\|_\infty \le \Delta t\sum_{k=0}^{M-1} C_{k+1,\Delta t,\eta}\, h.$$

Finally,

$$\sup_{0\le n\le M} \|e_h^n\|_\infty \le C_{\Delta t,\eta}\, h, \tag{3.13}$$

where $C_{\Delta t,\eta} = \Delta t\sum_{k=0}^{M-1} C_{k+1,\Delta t,\eta}$. □

3.3.2. Numerical tests

We present here the results obtained using either the first-order finite difference scheme (3.10) or the Crank-Nicolson method (see Appendix B for details).

For both schemes, we compare the numerical solutions to the exact solution of problem (3.8) with $\alpha = 1$, $g(x_l, t) = 2(1 - e^{-10t})$ and $g(x_r, t) = 3(1 - e^{-10t})$, see Figure 5. We choose $d = 0.1$ and $\Delta_l = \Delta_r = 0.3d$.

Setting the final time $T = 1$, we measure the error $\|\mathcal{V}_h(T) - U_h^M\|$ inside the fluid domain $[0, x_l] \cup [x_r, 1]$, where $\mathcal{V}_h(T) = (u(x_1, T), \ldots, u(x_N, T))^T$, as a function of Δt, η and h. Since

$$\|\mathcal{V}_h(T) - U_h^M\| \leq \|\mathcal{V}_h(T) - \mathcal{V}_h^M\| + \|\mathcal{V}_h^M - \mathcal{U}_h^M\| + \|\mathcal{U}_h^M - U_h^M\|,$$

where $\mathcal{V}_h^M = (u^M(x_1), \ldots, u^M(x_N))^T$ and $\mathcal{U}_h^M = (u_\eta^M(x_1), \ldots, u_\eta^M(x_N))^T$, three sources of error can be distinguished: $\|\mathcal{V}_h(T) - \mathcal{V}_h^M\|$ is an error related to the time discretization, $\|\mathcal{V}_h^M - \mathcal{U}_h^M\|$ is an error introduced by the penalization, and $\|\mathcal{U}_h^M - U_h^M\|$ is an error associated with the space discretization.

Formally one has

$$\|\mathcal{V}_h(T) - U_h^M\|_\infty \leq C\Delta t^q + C_{\Delta t}\eta + C_{\Delta t,\eta} h^p,$$

for a scheme of order p in space and order q in time, if the space discretization is adapted to the obstacle.

The above estimates are confirmed numerically by plotting the error inside the fluid domain. The orders of convergence are recovered (Figure 5(c) and Figure 5(d)). These tests suggest that the constants $C_{\Delta t}$ and $C_{\Delta t,\eta}$ remain bounded when $\Delta t, \eta \to 0$. Moreover, the implicit Euler scheme or the Crank-Nicolson scheme which are unconditionally stable (in the norms $\|\cdot\|_\infty$ and $\|\cdot\|_2$ for the former, in the norm $\|\cdot\|_2$ for the latter, when used to solve the heat equation) eliminate the need of a stability condition that could be very restrictive in practice in the context of penalization. Indeed, the penalization parameter η is intended to go to 0 introducing convective terms that dominate the diffusive one. It is therefore expected that the use of a fully explicit discretization for the penalization terms leads to a CFL (Courant-Friedrichs-Lewy) stability condition of the form $\frac{1}{\eta}\Delta t \leq \Delta x$.

4. Application

4.1. Nonlinear problem

The developed penalization method is here applied to a nonlinear advection-diffusion problem coming from a simplification of the model of electronic and ionic temperatures evolution along a magnetic field line, for a plasma in contact with an obstacle [9, 23]. It

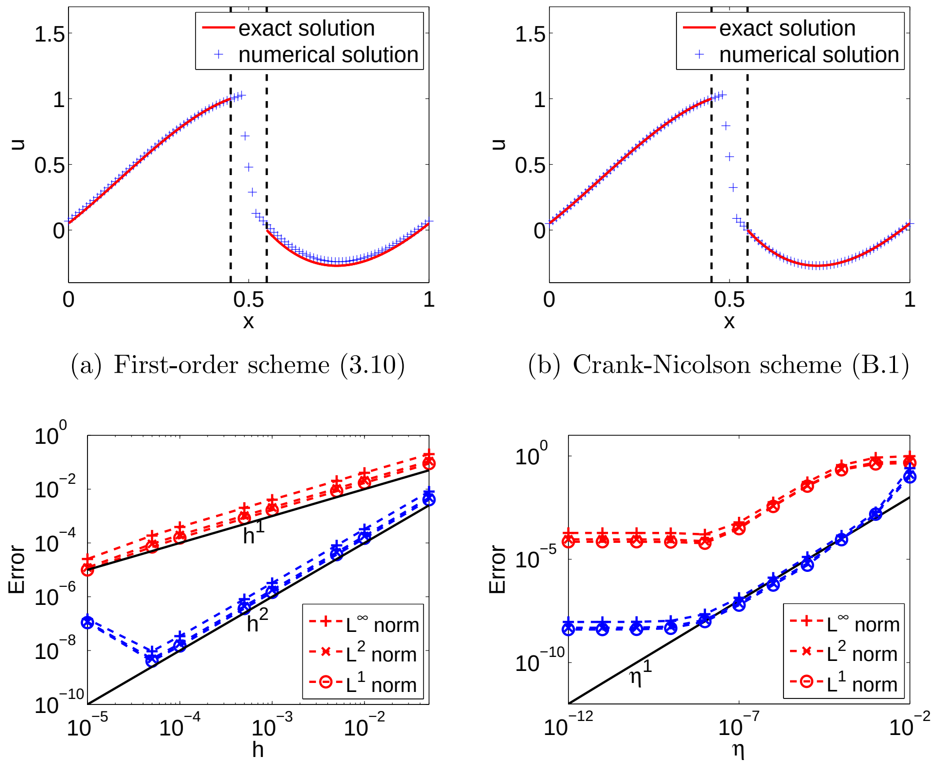

(a) First-order scheme (3.10)

(b) Crank-Nicolson scheme (B.1)

(c) $\Delta t = 10^{-4}$, $\eta = 10^{-10}$

(d) $\Delta t = 10^{-4}$, $h = 5 \times 10^{-5}$

Figure 5: Comparison between the numerical solution of the penalized parabolic problem and the exact solution of the original problem (3.8) with Robin boundary conditions at $T = 1$. (a)-(b): $\Delta t = 10^{-3}$, $\eta = 10^{-10}$ and $h = 10^{-2}$. Errors versus h (c) and errors versus η (d) for first-order (red) and Crank-Nicolson (blue) schemes.

reads:

$$
\begin{cases}
\dfrac{\partial u}{\partial t} + \dfrac{\partial}{\partial x}\big(v(x)u\big) = \nu \dfrac{\partial}{\partial x}\Big(u^{5/2}\dfrac{\partial u}{\partial x}\Big) + f & x \in]0, x_l[\cup]x_r, 1[,\ t \in]0, T[\\
u^{5/2}\dfrac{\partial u}{\partial x}(x_l, t) + \alpha u(x_l, t) = g(x_l, t) & t \in]0, T[\\
-u^{5/2}\dfrac{\partial u}{\partial x}(x_r, t) + \alpha u(x_r, t) = g(x_r, t) & t \in]0, T[\\
u(0, t) = u(1, t),\ \dfrac{\partial u}{\partial x}(0, t) = \dfrac{\partial u}{\partial x}(1, t) & t \in]0, T[\\
u(x, 0) = u_0(x) & x \in]0, x_l[\cup]x_r, 1[.
\end{cases}
\tag{4.1}
$$

According to the previous approach, we propose the following discretization:

$$
\begin{cases}
\dfrac{U_i^{n+1}-U_i^n}{\Delta t} + \dfrac{F_{i+1/2}(U^n)-F_{i-1/2}(U^n)}{h} \\
\qquad + \dfrac{\chi_l(x_i)}{\eta}\Big((U_i^n)^{5/2}\dfrac{U_i^{n+1}-U_{i-1}^{n+1}}{h} + \alpha U_i^{n+1} - g_l^{n+1}\Big) \\
\qquad + \dfrac{\chi_r(x_i)}{\eta}\Big(-(U_i^n)^{5/2}\dfrac{U_{i+1}^{n+1}-U_i^{n+1}}{h} + \alpha U_i^{n+1} - g_r^{n+1}\Big) \\
\qquad = \dfrac{\nu}{h}\Big(m_{i+1/2}(U^n)\dfrac{U_{i+1}^{n+1}-U_i^{n+1}}{h} - m_{i-1/2}(U^n)\dfrac{U_i^{n+1}-U_{i-1}^{n+1}}{h}\Big) \\
\qquad + (1-\chi(x_i))f(x_i,t^{n+1}) \\
U_0^{n+1} = U_N^{n+1},\ U_1^{n+1} = U_{N+1}^{n+1} \\
U_i^0 = (1-\chi(x_i))u_0(x_i) + \chi(x_i),
\end{cases} \tag{4.2}
$$

for $i = 1, \dots, N$ $(Nh = 1)$ and $n = 0, \dots, M-1$ $(M\Delta t = T)$.

The advection term is treated explicitly using an upwind scheme with:

$$
F_{i+1/2}(U^n) = \begin{cases} v_\chi(x_{i+1/2})U_i^n & \text{if } v_\chi(x_{i+1/2}) \geq 0 \\ v_\chi(x_{i+1/2})U_{i+1}^n & \text{if } v_\chi(x_{i+1/2}) < 0, \end{cases}
$$

$v_\chi(x)$ referring to $(1-\chi(x))v(x)$. The nonlinear penalization terms are treated semi-implicitly using an upwind scheme, while the nonlinear diffusion term is discretized semi-implicitly with:

$$
m_{i+1/2}(U^n) = \frac{1}{2}\big((U_i^n)^{5/2} + (U_{i+1}^n)^{5/2}\big).
$$

The temperature u is initialized to $u_0 = 1$ throughout the computational domain $[0,1]$ and we compare the numerical solution obtained by the scheme (4.2) with an exact stationary solution u_s of (4.1).

Figure 6(a) shows the numerical solution at $T = 10$ when the stationary state has been reached. The errors plotted in Figures 6(b) and 6(c) correspond to $\|\mathcal{V}_{s,h} - U_h^M\|$ in the fluid domain, where $\mathcal{V}_{s,h} = (u_s(x_1), \dots, u_s(x_N))^T$ and $U_h^M = (U_1^M, \dots, U_N^M)^T$. A first order of convergence is obtained with respect to the space step h (Figure 6(b)), which is consistent with the discretization (4.2). Depending on the penalization parameter η, a first order is observed (Figure 6(c)), as in the linear case.

According to these results, the penalization method proposed in this paper to enforce Neumann or Robin boundary conditions has been coupled with the penalization technique previously proposed in [16] for Dirichlet conditions. Numerical tests for a one-dimensional system of equations describing the density, the velocity and the temperature in the plasma of a tokamak close to an obstacle can be found in [23]. The present method is also implemented in a realistic two-dimensional code SolEdge2D dedicated to the simulation of the plasma-wall interaction in the edge region of a tokamak with complex geometries [9]. Extension of this method for the boundary conditions associated with electric potential has been sketched in [6].

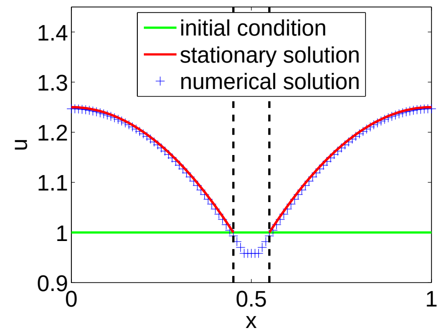

(a) $\Delta t = 10^{-3}$, $\eta = 10^{-10}$, $h = 10^{-2}$

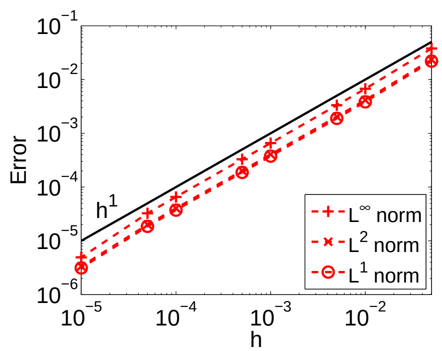

(b) $\Delta t = 10^{-3}$, $\eta = 10^{-10}$

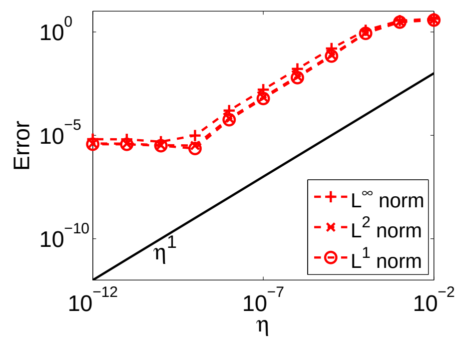

(c) $\Delta t = 10^{-3}$, $h = 10^{-5}$

Figure 6: (a): Comparison between numerical and exact stationary solutions at $T = 10$ for nonlinear problem (4.1). (b): Errors versus h. (c): Errors versus η.

4.2. Bivariate case

The difficulties faced when generalizing the approach to the multivariate case are real. The extension of various terms from the boundary to the complementary domain is one of the key difficulties.

To test the feasibility of the generalization, we consider the following problem:

$$\begin{cases} -\Delta u + u = f \quad \text{in } \omega \\ \dfrac{\partial u}{\partial n} + \alpha u = g \quad \text{on } \partial D \\ u(0, y) = u(1, y), \;\; u(x, 0) = u(x, 1), \end{cases} \tag{4.3}$$

where $D = D((x_0, y_0), r)$ is an open disk of center (x_0, y_0) and radius r included in $]0, 1[\times]0, 1[$ and $\omega =]0, 1[\times]0, 1[\setminus \bar{D}$. We propose the penalized problem:

$$\begin{cases} -\Delta u_\eta + u_\eta + \dfrac{\chi_0}{\eta}\big(\nabla u_\eta \cdot \tilde{n} + \alpha u_\eta - \tilde{g}\big) = (1 - \chi) f \quad \text{in } \Omega \\ u_\eta(0, y) = u_\eta(1, y), \;\; u_\eta(x, 0) = u_\eta(x, 1), \end{cases} \tag{4.4}$$

where $\Omega =]0, 1[\times]0, 1[$, $\eta > 0$ is the penalization parameter, χ is the characteristic function of D and χ_0 is the characteristic function of the ring $R = D \setminus \bar{D}_{\text{int}}$, $D_{\text{int}} = D((x_0, y_0), r_{\text{int}})$

being the open disk of center (x_0, y_0) and radius $0 < r_{\text{int}} < r$ (see Figure 7(a)). Finally, $\tilde{n}$ (resp. $\tilde{g}$) is an extension of n (resp. g) defined as follows:

$$\tilde{n}(x,y) = -\frac{\nabla\phi}{\|\nabla\phi\|} \quad \text{with} \quad \phi(x,y) = (x-x_0)^2 + (y-y_0)^2,$$
$$\tilde{g}(x,y) = g((x_0,y_0) + re^{i\theta}) \quad \text{with} \quad \theta = \arg\left((x-x_0) + i(y-y_0)\right).$$

Assuming the existence and uniqueness of the solution u_η of the penalized problem (4.4), we guess to have, in the limit $\eta \to 0$, the convergence $u_\eta \to \bar{u}$ such that:

- in ω, $\bar{u} = u$ solution of the original problem (4.3),
- in R, $\bar{u} = u_R$ solution of

$$\begin{cases} \nabla v \cdot \tilde{n} + \alpha v = \tilde{g} & \text{in } R \\ v = u & \text{on } \partial D, \end{cases}$$

- in D_{int}, $\bar{u} = u_{\text{int}}$ solution of

$$\begin{cases} -\Delta v + v = 0 & \text{in } D_{\text{int}} \\ v = u_R & \text{on } \partial D_{\text{int}}. \end{cases}$$

We present here the first numerical experiments performed to test the convergence of u_η to u in the original domain ω. The numerical test is made with a manufactured solution by choosing u 1-periodic in x and y and adjusting f and g accordingly. The numerical solution of the penalized problem obtained for $u(x,y) = \sin(2\pi x)\sin(2\pi y)$, $\alpha = 1$, $(x_0, y_0) = (0.6, 0.7)$, $r = 0.25$ and $r_{\text{int}} = 0.125$ is reported in Figure 7(c). The penalized problem is solved numerically using the finite element method provided by the FreeFem++ software [15]. On Figure 7(d), we report the L^2 norm error $\|u - u_{\eta,h}\|_{L^2(\omega)}$ for a fixed penalization parameter $\eta = 10^{-4}$ and different mesh sizes h. We observe a decrease of this error when $h \to 0$ showing numerically the convergence of the proposed method. The remaining error for the smallest h indicates that $u_\eta \approx u$ for the fixed value of $\eta \ll 1$.

5. Conclusion

A new penalization fictitious domain method to take account of Neumann or Robin boundary conditions has been proposed in this paper. This method has been first defined and analyzed for univariate linear partial differential equations of elliptic or parabolic types. Theoretical results including the convergence with respect to the penalization parameter η have been obtained. We then analyzed the convergence of finite difference discretization schemes of the penalized problem. We validated the method by various numerical tests that confirmed the theoretical results. This penalization method has been successfully applied to a nonlinear advection-diffusion equation mimicking the equations governing ionic and electronic temperatures of a plasma in the edge region of a tokamak. The first extension of this method to the multivariate case is finally reported.

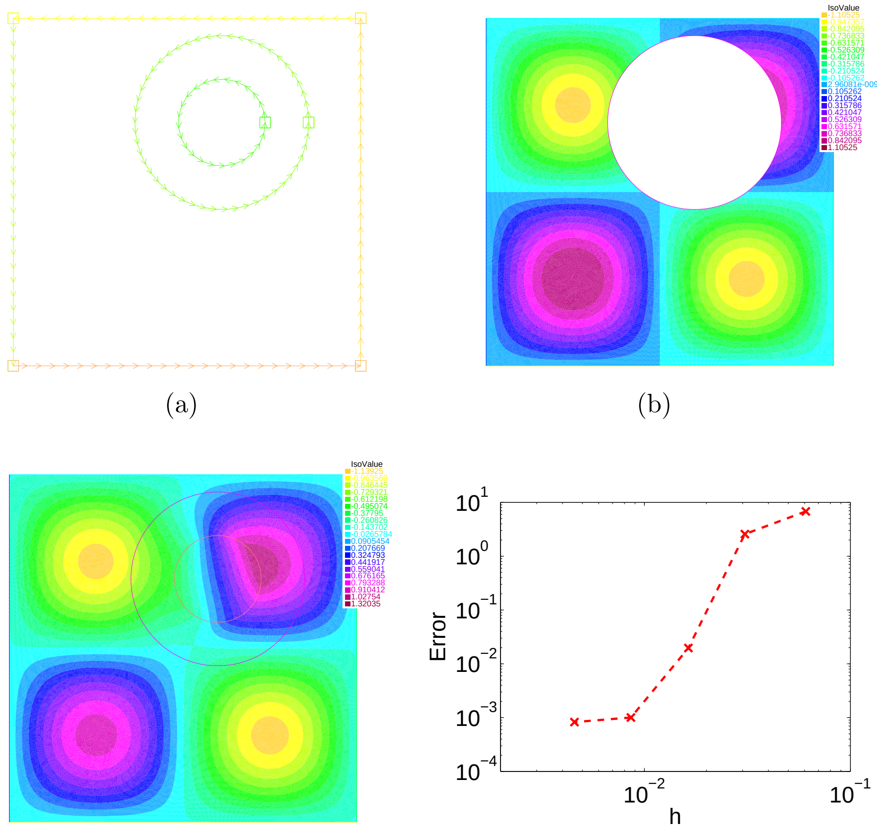

(a) (b)

(c) $\eta = 10^{-4}$, $h = 0.0163625$ (d) $\eta = 10^{-4}$

Figure 7: Comparison between the numerical solution (c) of the penalized problem (4.4), using the P^2 finite element method, and the exact solution (b) of the original problem (4.3). (a): Sketch of the domain. (d): L^2 errors versus h.

Acknowledgments

This work was supported by the Research Federation “Fusion par Confinement Magnétique - ITER” and the “ESPOIR” project (ANR-09-BLAN-0035-01, `http://sites.google.com/site/anrespoir/`).

Appendix A. Proof of Lemma 3.1

Proof. First, we reduce the inhomogeneous boundary conditions in (3.1) to homogeneous boundary conditions using the inverse trace theorem. According to [21, Theorem 8.3] (see also [8]), there exists a continuous operator $\mathcal{R}\colon H^{3/2}(\partial\omega) \times H^{1/2}(\partial\omega) \to H^2(\omega)$ such that $\mathcal{R}(h_1, h_2)|_{\partial\omega} = h_1$ and $\frac{\partial}{\partial n}\mathcal{R}(h_1, h_2)|_{\partial\omega} = h_2$. Thus, for all $t \in [0, T]$, there exists $v(t) = \mathcal{R}(0, g(t)) \in H^2(\omega)$ satisfying $v(t)|_{\partial\omega} = 0$ and $\frac{\partial v(t)}{\partial n}|_{\partial\omega} = g(t)$, so that $\frac{\partial v}{\partial n} + \alpha v = g$ on

$\partial\omega\times]0,T[$. Putting $u = v + w$, the equation (3.1) can be formally rewritten as

$$\begin{cases} \dfrac{\partial w}{\partial t} - \Delta w = f - \dfrac{\partial v}{\partial t} + \Delta v & \text{in } \omega\times]0,T[\\ \dfrac{\partial w}{\partial n} + \alpha w = 0 & \text{on } \partial\omega\times]0,T[\\ w(x,0) = u_0(x) - v(x,0) & \text{in } \omega. \end{cases} \tag{A.1}$$

Let us put $f^* = f - \frac{\partial v}{\partial t} + \Delta v$ and $u_0^* = u_0 - v(0)$. We want to show that $f^* \in L^2(]0,T[;L^2(\omega))$ and $u_0^* \in L^2(\omega)$. In order to do this, let us show that $v \in C^1([0,T];H^2(\omega))$. Noting $v_d(t) = \mathcal{R}\big(0, \frac{dg}{dt}(t)\big)$, there exists, by continuity of the operator $\mathcal{R}$, a constant $C \geq 0$ such that for all $t, t_0 \in [0,T]$ with $t \neq t_0$,

$$\left\| \frac{v(t) - v(t_0)}{t - t_0} - v_d(t) \right\|_{H^2(\omega)} \leq C \left\| \frac{g(t) - g(t_0)}{t - t_0} - \frac{dg}{dt}(t) \right\|_{H^{1/2}(\omega)}. \tag{A.2}$$

Letting t go to t_0 in (A.2), we deduce the differentiability of v and $\frac{dv}{dt}(t) = v_d(t) = \mathcal{R}\big(0, \frac{dg}{dt}(t)\big)$. The continuity of $\frac{dv}{dt}$ then follows similarly from the inequality

$$\left\| \frac{dv}{dt}(t) - \frac{dv}{dt}(t_0) \right\|_{H^2(\omega)} \leq C \left\| \frac{dg}{dt}(t) - \frac{dg}{dt}(t_0) \right\|_{H^{1/2}(\omega)}. \tag{A.3}$$

Hence $v \in C^1([0,T];H^2(\omega))$, in particular $v(0) \in L^2(\omega)$, $\frac{\partial v}{\partial t} \in L^2(]0,T[;L^2(\omega))$ and $\Delta v \in L^2(]0,T[;L^2(\omega))$. Thus $f^* \in L^2(]0,T[;L^2(\omega))$ and $u_0^* \in L^2(\omega)$.

Second, we show that the equation

$$\begin{cases} \dfrac{\partial w}{\partial t} - \Delta w = f^* & \text{in } \omega\times]0,T[\\ \dfrac{\partial w}{\partial n} + \alpha w = 0 & \text{on } \partial\omega\times]0,T[\\ w(x,0) = u_0^*(x) & \text{in } \omega, \end{cases} \tag{A.4}$$

where $f^* \in L^2(]0,T[;L^2(\omega))$ and $u_0^* \in L^2(\omega)$, has a unique solution w in the space $L^2(]0,T[;H^1(\omega))\cap C^0([0,T];L^2(\omega))$. Introducing a new unknown function $w^*(t) = e^{-t}w(t)$, (A.4) is equivalent to

$$\begin{cases} \dfrac{\partial w^*}{\partial t} - \Delta w^* + w^* = f^{**} & \text{in } \omega\times]0,T[\\ \dfrac{\partial w^*}{\partial n} + \alpha w^* = 0 & \text{on } \partial\omega\times]0,T[\\ w^*(x,0) = u_0^{**}(x) & \text{in } \omega, \end{cases} \tag{A.5}$$

where $f^{**} = f^* e^{-t} \in L^2(]0,T[;L^2(\omega))$ and $u_0^{**} = u_0^* \in L^2(\omega)$. We consider the following weak formulation of (A.5):

$$\left| \begin{array}{l} \text{Find } w^* \in L^2(]0,T[;H^1(\omega)) \cap C^0([0,T];L^2(\omega)) \text{ such that} \\ \begin{cases} \dfrac{d}{dt}\langle w^*(t), v\rangle_{L^2(\omega)} + a(w^*(t), v) = \langle f^{**}(t), v\rangle_{L^2(\omega)} \quad \forall v \in H^1(\omega) \\ \qquad\qquad \text{(in distributional sense in }]0,T[) \\ w^*(t=0) = u_0^{**}, \end{cases} \end{array} \right. \tag{A.6}$$

where

$$
\begin{aligned}
\forall u, v \in H^1(\omega), \quad & a(u,v) = \int_\omega \nabla u \cdot \nabla v \, dx + \int_\omega uv \, dx + \alpha \int_{\partial\omega} uv \, d\sigma, \\
\forall u, v \in L^2(\omega), \quad & \langle u, v \rangle_{L^2(\omega)} = \int_\omega uv \, dx.
\end{aligned}
$$

Applying [1, Theorem 8.2.3] (whose proof is based on a spectral approach) yields the existence and uniqueness of the solution $w^* \in L^2(]0,T[; H^1(\omega)) \cap C^0([0,T]; L^2(\omega))$ of the weak formulation (A.6). $\square$

Appendix B. The Crank-Nicolson method used in Section 3.3.2

The Crank-Nicolson method is applied directly to the continuous penalization of the original problem (3.8) providing the following scheme:

$$
\begin{cases}
\dfrac{U_i^{n+1} - U_i^n}{\Delta t} + \dfrac{1}{2}\Big[-\dfrac{U_{i+1}^{n+1} - 2U_i^{n+1} + U_{i-1}^{n+1}}{h^2} \\
\qquad + \dfrac{\chi_l(x_i)}{\eta}\Big(\dfrac{3U_i^{n+1} - 4U_{i-1}^{n+1} + U_{i-2}^{n+1}}{2h} + \alpha U_i^{n+1} - g_l^{n+1} \Big) \\
\qquad + \dfrac{\chi_r(x_i)}{\eta}\Big(-\dfrac{-U_{i+2}^{n+1} + 4U_{i+1}^{n+1} - 3U_i^{n+1}}{2h} + \alpha U_i^{n+1} - g_r^{n+1} \Big) \\
\qquad - \dfrac{U_{i+1}^{n} - 2U_i^{n} + U_{i-1}^{n}}{h^2} \\
\qquad + \dfrac{\chi_l(x_i)}{\eta}\Big(\dfrac{3U_i^{n} - 4U_{i-1}^{n} + U_{i-2}^{n}}{2h} + \alpha U_i^{n} - g_l^{n} \Big) \\
\qquad + \dfrac{\chi_r(x_i)}{\eta}\Big(-\dfrac{-U_{i+2}^{n} + 4U_{i+1}^{n} - 3U_i^{n}}{2h} + \alpha U_i^{n} - g_r^{n} \Big) \Big] \\
\qquad = \dfrac{1}{2}(1 - \chi(x_i))\big(f(x_i, t^{n+1}) + f(x_i, t^n) \big) \\
U_i^{n+1} = U_{N+i}^{n+1} \\
U_i^0 = (1 - \chi(x_i)) u_0(x_i),
\end{cases}
\tag{B.1}
$$

for $i = 1, \ldots, N$ and $n = 0, \ldots, M-1$.

References

[1] G. Allaire, Analyse numérique et optimisation : une introduction à la modélisation mathématique et à la simulation numérique, Éd. de l'École Polytechnique, 2005.

[2] P. Angot, A unified fictitious domain model for general embedded boundary conditions, C. R. Acad. Sci. Paris, Ser. I 341 (2005) 683–688.

[3] P. Angot, T. Auphan, O. Guès, An optimal penalty method for a hyperbolic system modeling the edge plasma transport in a tokamak, J. Comput. Phys. 261 (2014) 1–22.

[4] P. Angot, C.H. Bruneau, P. Fabrie, A penalization method to take into account obstacles in incompressible viscous flows, Numer. Math. 81 (1999) 497–520.

[5] E. Arquis, J.P. Caltagirone, Sur les conditions hydrodynamiques au voisinage d'une interface milieu fluide-milieux poreux : application à la convection naturelle, C. R. Acad. Sci. Paris, Ser. II 299 (1984) 1–4.

[6] T. Auphan, Analyse de modèles pour ITER; Traitement des conditions aux limites de systèmes modélisant le plasma de bord dans un tokamak, Ph.D. thesis, Aix-Marseille Université, 2014.

[7] F. Boyer, Approximation numérique complète d'un problème parabolique, `http://www.latp.univ-mrs.fr/~fboyer/Enseignement/M2_AN/examen0910.pdf` [Online ; accessed 29-July-2014], 2009-2010. Numerical Analysis exam of M2 PDE and Scientific Computing, Marseille.

[8] F. Boyer, P. Fabrie, Eléments d'analyse pour l'étude de quelques modèles d'écoulements de fluides visqueux incompressibles, Springer, 2006.

[9] H. Bufferand, B. Bensiali, J. Bucalossi, G. Ciraolo, P. Genesio, P. Ghendrih, Y. Marandet, A. Paredes, F. Schwander, E. Serre, P. Tamain, Near wall plasma simulation using penalization technique with the transport code SolEdge2D-Eirene, J. Nucl. Mater. 438 (2013) S445–S448. Proceedings of the 20th International Conference on Plasma-Surface Interactions in Controlled Fusion Devices.

[10] Q. Chen, Y. Hong, R. Temam, Analysis of a penalty method, J. Sci. Comput. 53 (2012) 3–34.

[11] R. Dautray, J.L. Lions, Analyse mathématique et calcul numérique pour les sciences et les techniques, volume 4 : Méthodes variationnelles, Masson, 1988.

[12] R. Dautray, J.L. Lions, Analyse mathématique et calcul numérique pour les sciences et les techniques, volume 7 : Évolution : Fourier, Laplace, Masson, 1988.

[13] B. Fornet, A Kreiss' symmetrizer domain penalization method, Comm. Partial Differential Equations 33 (2008) 1549–1570.

[14] B. Fornet, O. Guès, Penalization approach to semi-linear symmetric hyperbolic problems with dissipative boundary conditions, Discrete Contin. Dynam. Systems 23 (2009) 827–845.

[15] F. Hecht, New development in freefem++, J. Numer. Math. 20 (2012) 251–265.

[16] L. Isoardi, G. Chiavassa, G. Ciraolo, P. Haldenwang, E. Serre, P. Ghendrih, Y. Sarazin, F. Schwander, P. Tamain, Penalization modeling of a limiter in the tokamak edge plasma, J. Comput. Phys. 229 (2010) 2220–2235.

[17] B. Kadoch, D. Kolomenskiy, P. Angot, K. Schneider, A volume penalization method for incompressible flows and scalar advection-diffusion with moving obstacles, J. Comput. Phys. 231 (2012) 4365–4383.

[18] N.K.R. Kevlahan, J.M. Ghidaglia, Computation of turbulent flow past an array of cylinders using a spectral method with Brinkman penalization, Eur. J. Mech. B - Fluids 20 (2001) 333–350.

[19] N.K.R. Kevlahan, O.V. Vasilyev, An adaptive wavelet collocation method for fluid-structure interaction at high Reynolds numbers, SIAM J. Sci. Comput. 26 (2005) 1894–1915.

[20] K. Khadra, P. Angot, S. Parneix, J.P. Caltagirone, Fictitious domain approach for numerical modelling of Navier-Stokes equations, Int. J. Numer. Meth. Fluids 34 (2000) 651–684.

[21] J.L. Lions, E. Magenes, Problèmes aux limites non homogènes et applications, volume 1, Dunod, 1968.

[22] A. Paccou, G. Chiavassa, J. Liandrat, K. Schneider, A penalization method applied to the wave equation, C. R. Mécanique 333 (2005) 79–85.

[23] A. Paredes, H. Bufferand, F. Schwander, G. Ciraolo, E. Serre, P. Ghendrih, P. Tamain, Penalization technique to model wall-component impact on heat and mass transport in the tokamak edge, J. Nucl. Mater. 438 (2013) S625–S628. Proceedings of the 20th International Conference on Plasma-Surface Interactions in Controlled Fusion Devices.

[24] I. Ramière, P. Angot, M. Belliard, A fictitious domain approach with spread interface for elliptic problems with general boundary conditions, Comput. Methods Appl. Mech. Engrg. 196 (2007) 766–781.

[25] I. Ramière, P. Angot, M. Belliard, A general fictitious domain method with immersed jumps and multilevel nested structured meshes, J. Comput. Phys. 225 (2007) 1347–1387.

[26] K. Schneider, M. Farge, Adaptive wavelet simulation of a flow around an impulsively started cylinder using penalisation, Appl. Comput. Harmon. Anal. 12 (2002) 374–380.

[27] O.V. Vasilyev, N.K.R. Kevlahan, Hybrid wavelet collocation-Brinkman penalization method for complex geometry flows, Int. J. Numer. Meth. Fluids 40 (2002) 531–538.